



In-situ regeneration of a novel Fe₃O₄/GAC adsorbent for micropollutants removal in a continuous fixed-bed

Julia Nieto-Sandoval*, Ferdaus El Morabet, Macarena Munoz*, Neus Lopez-Arago, Zahara M. de Pedro, Jose A. Casas

Chemical Engineering Department, Universidad Autónoma de Madrid, Ctra. Colmenar km 15, Madrid 28049, Spain



ARTICLE INFO

Keywords:

Adsorption
Adsorbent regeneration
Water treatment
Activated carbon
Diclofenac

ABSTRACT

Adsorption onto activated carbon is one of the most feasible techniques for micropollutants removal from water. Nevertheless, the sustainability and economy of this process is strongly limited by the difficult regeneration of the saturated adsorbents, which, in practice, are commonly disposed. This work aims to tackle this challenge by the development of a granular activated carbon (GAC) decorated with magnetite nanoparticles (Fe₃O₄/GAC), that allows the *in-situ* regeneration of the saturated solid by H₂O₂ addition (through heterogeneous Fenton oxidation). Its performance was tested in a fixed-bed column in continuous operation using the pharmaceutical diclofenac (DCF) as target pollutant. The adsorbent was synthesized by the incorporation of 5% wt. iron to commercial granular activated carbon (GAC) by incipient wetness impregnation, followed by calcination and reduction. The immobilization of magnetite nanoparticles did not significantly alter neither the specific surface area (~1000 m² g⁻¹) nor the main properties of the solid, which was fully characterized. Accordingly, its adsorption capacity remained practically unchanged (~400 mg g⁻¹). Remarkably, the addition of H₂O₂ allowed to restore the adsorption capacity of the adsorbent at 25 °C using a H₂O₂ dose of 3 - 6 g L⁻¹ during 20 h. *In-situ* regeneration was demonstrated in three consecutive adsorption-regeneration runs for the treatment of 100 mg L⁻¹ DCF, obtaining similar breakthrough curves. Notably, iron leaching was practically negligible during operation and was below 2% wt. of the solid along the regeneration treatment. As a proof of concept, the feasibility of the system was finally proved in the treatment of a representative concentration of DCF (500 µg L⁻¹). The adsorbent led to the complete removal of the pollutant along 10 days and was effectively regenerated after saturation in just 3 h.

1. Introduction

The widespread occurrence of emerging pollutants in the aquatic ecosystems represents an important challenge for the scientific community (Luo et al., 2014). Such compounds *i.e.* pharmaceuticals, personal care products, pesticides, among others, are characterized by a high persistence and non-biodegradability character. Their presence provoke a potential risk to aquatic organisms, animals and human health, due to the impact of drinking water, even at the low concentrations detected (ng L⁻¹ or µg L⁻¹) (Bolong et al., 2009; Khan et al., 2022; Pereira et al., 2015). For instance, the anti-inflammatory drug diclofenac (DCF) bioaccumulation in a number of fish and invertebrate species has affected their growth, reproduction and metabolisms (Acuña et al., 2015). Furthermore, the cardiotoxicity, hepatotoxicity and genotoxicity of DCF in different mammalian systems have been confirmed (Sathishkumar et al., 2020). Although this emerging pollutant was included in the Watch List of EU Decision 2015/49, its permissible limit in the aquatic environment is still not regulated.

Efforts are growing with the aim of developing advanced processes that warrant the complete removal of these micropollutants at relevant facilities for both the environment and public health: Wastewater Treatment Plants (WWTPs) and Drinking Water Treatment Plants (DWTPs) (Rizzo et al., 2019). Among the alternatives explored, Advanced Oxidation Processes (AOPs) such as Fenton-based technologies, ozonation and photocatalysis are the main field of research nowadays (von Gunten, 2018; Yin and Shang, 2020). Nevertheless, these technologies are mainly available at lab-scale, being very scarce full-scale applications (Rout et al., 2021). In this context, adsorption is still considered the most plausible process for micropollutants removal, and in fact, this technology is increasingly being implemented as purification treatment in WWTPs and DWTPs of the European Union (Guillossou et al., 2019). Adsorption process stands out for its simple, inexpensive and ecofriendly operation (Shahid et al., 2021). Activated carbon (AC) is the most common used adsorbent due to its high porosity and surface area as well as low cost (Rodriguez-Narvaez et al., 2017). Powdered AC (PAC) has shown high adsorption efficiencies due to its large available

* Corresponding authors.

E-mail addresses: julia.nieto-sandoval@uam.es (J. Nieto-Sandoval), macarena.munoz@uam.es (M. Munoz).

<https://doi.org/10.1016/j.hazadv.2023.100267>

Received 19 December 2022; Received in revised form 1 February 2023; Accepted 22 February 2023

2772-4166/© 2023 The Authors. Published by Elsevier B.V. This is an open access article under the CC BY-NC-ND license (<http://creativecommons.org/licenses/by-nc-nd/4.0/>)

specific surface area but it can induce high pressure drops when used as packed bed in continuous processes and fine residues can become impurities in the treated effluent (Kårelid et al., 2017). Accordingly, granular AC (GAC) represents a more feasible alternative for water purification (Altmann et al., 2016).

The main limitation of the adsorption process is the management of saturated adsorbents (Larasati et al., 2020). Different strategies have been explored to regenerate the adsorbent material for further reusability (Lu et al., 2011; Wang et al., 2021; Zhou et al., 2021). However, most of these regeneration procedures lead to concentrated solutions of the pollutants, which requires further management (Hernández-Abreu et al., 2020; Larasati et al., 2020; Tan et al., 2009). Furthermore, they usually imply the use of organic solvents, which also represent a source of pollution. In this context, the Fenton oxidation process appears as a promising solution to solve this issue. This technology allows to degrade the concentrated pollutants in the adsorbent materials, desirably to biodegradable short-chain acids, CO₂ and water, avoiding the formation of additional concentrated solutions. In this sense, the homogeneous Fenton process has shown promising results in long-term operation for *in-situ* continuous GAC regeneration (Cai et al., 2020). However, in order to overcome its main limitations through the recovery and reuse of the catalyst, as well as avoid additional water pollution by dissolved iron salts, research efforts are focused on the employment of heterogeneous Fenton process. In this sense, new materials have been developed and applied mostly in batch mode heterogeneous Fenton showing promising results for the effectively regeneration of saturated adsorbents (Duan et al., 2020; Munoz et al., 2021). So, the *in-situ* regeneration of the adsorbent material in a fixed-bed column represents an important step forward for scale-up. In this sense, few works have dealt with the application of the heterogeneous Fenton process as a promising solution in continuous mode using carbonous based adsorbents (Bai et al., 2018; Song et al., 2015; Zhang et al., 2016). Nevertheless, most of them have reported a remarkable decrease in regeneration removal efficiencies after consecutive adsorption-regeneration applications, iron leaching from the developed adsorbent or severe operating conditions (Bai et al., 2018; Zhang et al., 2016). Accordingly, the development of an adsorbent that warrant the removal efficiency and keep the adsorption capacity after consecutive adsorption-regeneration by *in-situ* heterogeneous Fenton oxidation would overcome those limitations. Its suitability should be also demonstrated in continuous long-term operation (>100 h) which, so far, has not been explored in the literature.

This work aims to develop a regenerable GAC for the removal of micropollutants under continuous operation. The extensively consumed anti-inflammatory drug diclofenac (DCF) was selected as target compound given its high persistency and widespread occurrence in WWTP discharges (Barbosa et al., 2016). GAC was decorated with magnetite nanoparticles to obtain Fe₃O₄/GAC, whose adsorption properties were fully evaluated and compared with those of conventional GAC. The application of heterogeneous Fenton oxidation was afterwards evaluated to regenerate the saturated solid. Once determined the optimum regeneration conditions, the system was applied in a packed fixed-bed column, where *in-situ* regeneration was performed in consecutive adsorption-regeneration cycles. As a proof of concept, the system was investigated in the treatment of a more representative concentration of the target pollutant (500 mg L⁻¹) in long-term continuous operation *i.e.* 10 d before and after the regeneration, which just required 3 h.

2. Materials and methods

2.1. Materials

Diclofenac sodium salt (analytical standard), nitric acid (65%) and hydroxylamine (≥ 99%) were provided by Sigma-Aldrich. Hydrogen peroxide solution (30% w/v) and acetonitrile (99.9%) were supplied by Scharlau. Titanium oxysulfate (>99%) and 1,10-phenantroline were provided by Fluka. Iron (III) nitrate nonahydrate (98%) and acetic acid

(99.5%) were purchased from Panreac. Hydrogen (99.9%) and nitrogen (99.95) were obtained by Praxair. Deionized water was used to carry out all the experiments.

2.2. Synthesis and characterization of Fe₃O₄/GAC

The commercial granular activated carbon (GAC) used for the synthesis of Fe₃O₄/GAC was delivered by Chemviron (CAS nr.7440–44–0). Incipient wetness impregnation was applied for the incorporation of iron onto the carbon surface using iron (III) nitrate. The Fe load was adjusted to a nominal 5% wt. After impregnation, the material was left for 2 h at room temperature and dried for 12 h at 60 °C. The solid was then calcined for 4 h at 300 °C. The temperature was increased to that threshold value at a heating rate of 5 °C min⁻¹. Afterwards, the resulting material was submitted to a reduction stage in H₂ atmosphere for 2 h at 350 °C using 50 and 200 N mL min⁻¹ of hydrogen and nitrogen, respectively.

The porous structure of GAC and Fe₃O₄/GAC, previously outgassed overnight at 150 °C to a residual pressure of < 10⁻³ Torr, was characterized by nitrogen adsorption-desorption at -196 °C using a Micromeritics Tristar 3020 apparatus. Iron content was determined by Total reflection X Ray Fluorescence using a S2 PicoFox Bruker spectrometer. TAINstruments SDT650 apparatus was employed to evaluate the thermal stability of the materials in air. The magnetic properties of Fe₃O₄/GAC were determined by a superconducting quantum interference device (SQUID) (Quantum Design MPMS XL-5). X-ray diffraction (XRD) analysis was carried out using a Theta/2Theta Bruker D8 diffractometer. The point of zero charge (pH_{PZC}) of the adsorbents was determined following a method described elsewhere (Gomes et al., 2010). Briefly, 50 mg of the adsorbent were introduced in 5 mL of solutions varying initial pH (2–12) and the suspensions were left under stirring for 24 h. The pH_{PZC} value of each adsorbent was determined intercepting the obtained final pH versus initial pH curve with the straight line final pH = initial pH.

2.3. Adsorption tests

Adsorption experiments were carried out at 25 °C in 100 mL glass bottles shaken in a thermostatic bath (Julabo SW22) at 150 rpm. Both kinetic and equilibrium adsorption tests were performed to determine the equilibrium time and adsorption isotherms of the pharmaceutical DCF onto 15 mg of GAC and Fe₃O₄/GAC in 50 mL of solution. The initial concentration of DCF was fixed at 100 mg L⁻¹ in the kinetic runs while it was varied from 1 to 250 mg L⁻¹ in the equilibrium adsorption tests for 4 days. In preliminary experiments, it was confirmed this contact time allowed to reach the equilibrium. All experiments were carried out by triplicate and all data are expressed as the mean.

The equilibrium adsorption capacity of GAC and Fe₃O₄/GAC was calculated by the following Eq. (1):

$$q_e = \frac{(C_0 - C_e) \cdot V}{W} \quad (1)$$

where q_e (mg g⁻¹) is the equilibrium adsorption capacity; C_0 (mg L⁻¹) is the initial DCF concentration; C_e (mg L⁻¹) is the equilibrium DCF concentration; V (L) is the solution volume and W (g) is the adsorbent weight.

To get further insights on the adsorption tests, the pseudo-second order model, described by Ho (1995), was employed to describe the kinetic data. This model suggests that chemisorption controls the adsorption process (Ho and McKay, 1999). Accordingly, the following equation was used to fit the experimental data:

$$\frac{dq(t)}{dt} = k_2 (q_e - q(t))^2 \quad (2)$$

where $q(t)$ is the amount adsorbed at time t in mg g⁻¹, q_e (mg g⁻¹) is the equilibrium adsorption capacity and k_2 (g mg⁻¹ h⁻¹) is the pseudo-second-order rate constant. The integration of Eq. (2) was performed with the following initial values $t = 0$: $q(t) = 0$, obtaining Eq. (3) after

Table 1
Main properties of the adsorbents tested in this work.

	Fe (% wt.)	M _s (emu g ⁻¹)	S _{BET} (m ² g ⁻¹)	V _{mesopore} (cm ³ g ⁻¹)	V _{micropore} (cm ³ g ⁻¹)	pH _{PZC}
GAC	0.4	0	976	0.22	0.34	7.10
Fe ₃ O ₄ /GAC	5.1	0.13	995	0.31	0.24	6.50

rearrangement:

$$\frac{t}{q(t)} = \frac{1}{k_2 \cdot q_e} + \frac{t}{q_e} \quad (3)$$

2.4. Adsorbent regeneration procedure

Adsorbent regeneration runs were carried out with pre-saturated solids. To saturate the adsorbent, the adsorption test conditions were applied. The fresh solid (150 mg) was suspended in 500 mL of a DCF solution (100 mg L⁻¹) for 4 days at 25 °C in a thermostatic bath (150 rpm). Afterwards, the solution was filtrated and the solid was dried at 60 °C overnight. Regeneration tests were then carried out via Fenton oxidation (batch mode) by the treatment of the adsorbent (0.25 g L⁻¹) with an aqueous solution of H₂O₂ operating at pH₀ = 3 in a thermostatic bath (150 rpm) at 25 °C for 20 h. The H₂O₂ concentration was varied (1, 3 and 6 g L⁻¹) with the aim of optimizing the adsorption capacity restoration yield.

2.5. Fixed-bed adsorption experiments

A preliminary study was firstly carried out to select the optimum conditions for the adsorption experiments (*i.e.* column internal diameter, adsorbent weight and inlet flow). Packed-bed adsorption experiments were conducted using a glass column of 4 mm internal diameter and 30 cm length. The column was packed with 0.5 g of Fe₃O₄/GAC, which corresponds to 8.5 cm bed length, sieved within a range of 150 to 315 μm particle size to avoid preferential paths. The column extremes were filled with a layer of glass wool and glass spheres to compact the adsorbent and to avoid dead volumes and preferential pathways. The influent (100 mg DCF L⁻¹) was fed at 3 mL min⁻¹ in an up-flow direction using an Ismatec multichannel peristaltic pump (model ISM597D) and breakthrough curves were obtained. Once saturated, the adsorbent was *in-situ* regenerated by pumping a solution of H₂O₂ (6 g L⁻¹) at pH₀ = 3 for 3 h under ambient conditions. After the regeneration procedure, the adsorbent was flushed with distilled water for 10 min prior to the next adsorption cycle. To further demonstrate the feasibility of the system, long-term experiments with short (3 h) regeneration breaks were carried out using representative DCF streams (500 μg L⁻¹).

Although the most common mathematical model used to describe breakthrough data in the literature are Adams-Bohart and Thomas models (Bohart and Adams, 1920; Thomas, 1944), the well-known Modified dose-response model (MDR) was selected to describe the S-shaped curve of breakthrough obtained in this work as it yielded the best fitting results. This model, introduced more recently by Yan et al. (2001), minimizes the errors from Thomas model, particularly at very short and long operation times (de Andrade et al., 2020; Yan et al., 2001). Yan model was applied according to Eq. (4):

$$\frac{C}{C_0} = 1 - \frac{1}{1 + \left(\frac{C_0 \cdot Q \cdot t}{q_Y \cdot W} \right)} \quad (4)$$

where q_Y (mg g⁻¹) is the amount of solute adsorbed and a_Y is the Yan model rate constant.

2.6. Analytical methods

Liquid samples were periodically taken in both batch and continuous experiments, and immediately analyzed after adsorbent separation using PTFE filters (0.45 μm). DCF concentration was quantified

by HPLC-UV (Shimadzu, Prominence-i model, LC-2030C LT) using an Agilent Eclipse Plus C18 column (15 cm length, 4.6 mm diameter) as stationary phase. Analyses were performed at 270 nm using a 57/43% (v/v) mixture of acetonitrile and acetic acid aqueous solution (75 mM) as mobile phase. Dissolved iron concentration was quantified by colorimetry with a UV 2100 Shimadzu UV-VIS spectrophotometer using the o-phenantroline method (Sandell, 1959).

3. Results and discussion

3.1. Adsorbents characterization

Table 1 summarizes the main properties of the adsorbent synthesized in this work (Fe₃O₄/GAC) and those of the commercial GAC used as precursor. As can be seen, both materials showed a high specific surface area value, around 1000 m² g⁻¹, which is common for conventional activated carbons (Bhadra et al., 2016; Hasan et al., 2016; Rakić et al., 2015). Remarkably, the incorporation of magnetite nanoparticles did not lead to any reduction on the specific surface area of the solids. In fact, both isotherms were quite similar (see Fig. 1a) and corresponded to type I, typical of microporous materials.

TXRF analyses of GAC and Fe₃O₄/GAC revealed the low iron content of the commercial carbon (0.4% wt.) and confirmed the successful incorporation of iron in the synthesized material by incipient wetness impregnation, achieving the nominal 5% wt. These results are consistent with thermogravimetric analyses (see Fig. S2 of the Supplementary Material). A significant reduction of the adsorbents weight due to carbon oxidation was observed at 500 °C for GAC (90% reduction). In the case of Fe₃O₄/GAC, the presence of iron catalyzed the oxidation of carbon and thus, the loss of weight mainly occurred at 400°C (85% reduction). It must be noted that iron was mainly as Fe₃O₄ in the adsorbent developed in this work as it showed magnetic properties (Fig. 1b). In fact, XRD pattern of the Fe₃O₄/GAC allowed to identify Fe₃O₄ phase (see Fig. S3 of the Supplementary Material). Although Fe₂O₃ phase was also presented in the material, due to the thermal reduction treatment that led to clear magnetic properties to the material (Muñoz et al., 2013), Fe₃O₄ was the main phase present. On the other hand, both GAC and Fe₃O₄/GAC materials exhibited pH_{PZC} values close to 7 (Figs. 1c and S1 of the Supplementary Material), which led to a neutral superficial charge according to the aqueous medium pH.

3.2. Adsorption capacity

The adsorption isotherms of DCF onto GAC and Fe₃O₄/GAC adsorbents are depicted in Fig. 2. The initial micropollutant concentration was varied in the range from 1 to 250 mg L⁻¹ and the adsorbent dose was fixed at 0.3 mg mL⁻¹. In both cases, a clear sigmoidal shape was observed and thus, the isotherms can be categorized as Type II according to Brunauer's classification. This fact is indicative of the existence of multilayers at the internal surface of a material (Blahovec and Yantiotis, 2009). The adsorption capacity values achieved by GAC and Fe₃O₄/GAC at the maximum initial concentration of DCF (250 mg L⁻¹) were 368 and 379 mg g⁻¹, respectively. Therefore, it can be confirmed that the incorporation of magnetite nanoparticles did not lead to any negative impact on the GAC adsorption capacity. Thus, the low amount of Fe introduced in the adsorbent (5% wt.) allows to maintain the outstanding properties of the GAC support *viz.* specific surface area value (~1000 m² g⁻¹) and adsorption capacity (~400 mg g⁻¹) of the solid in

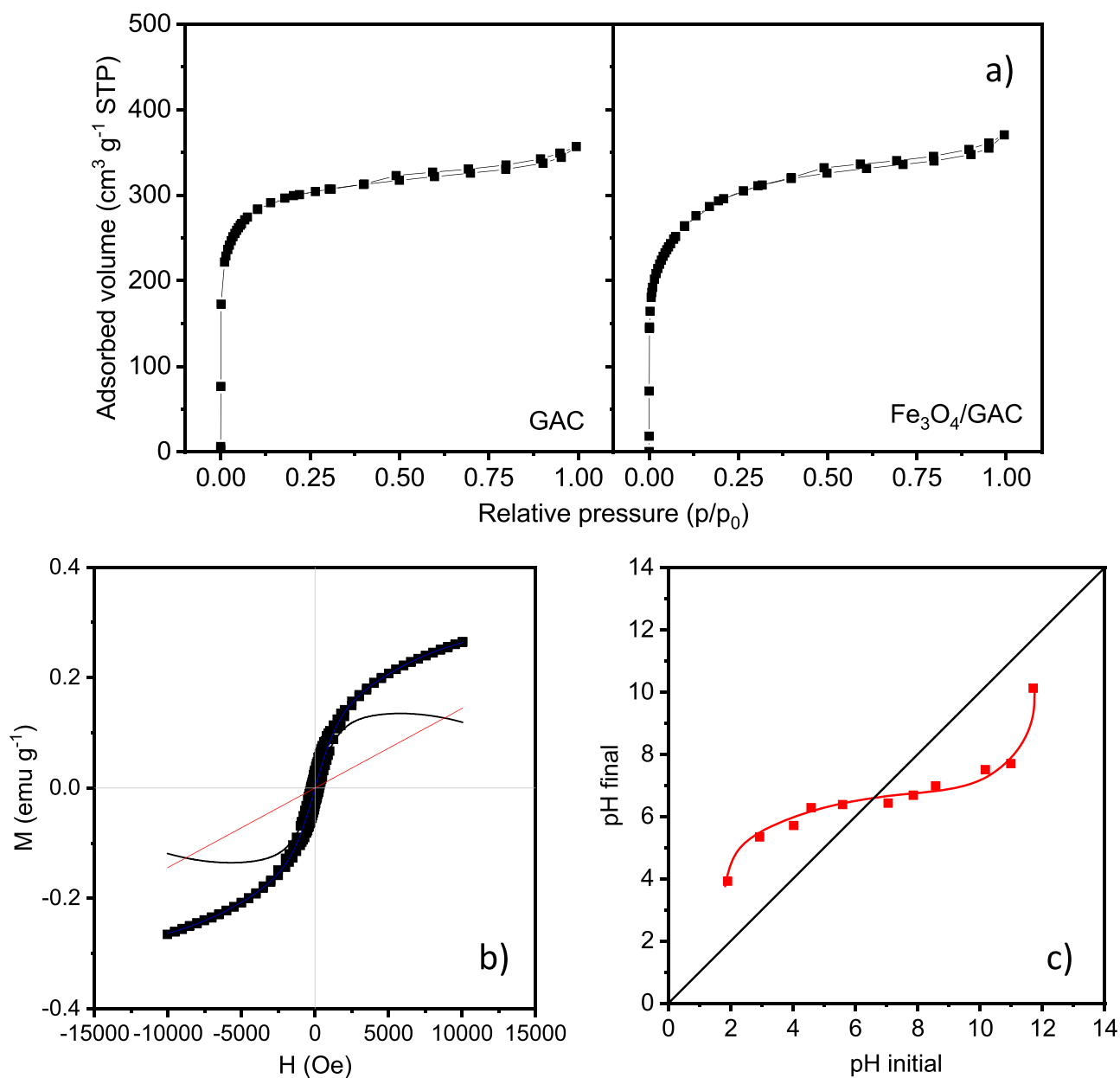


Fig. 1. N₂ adsorption-desorption isotherm of GAC and Fe₃O₄/GAC (a), magnetization hysteresis loop (b) and pH_{pzc} of Fe₃O₄/GAC (c).

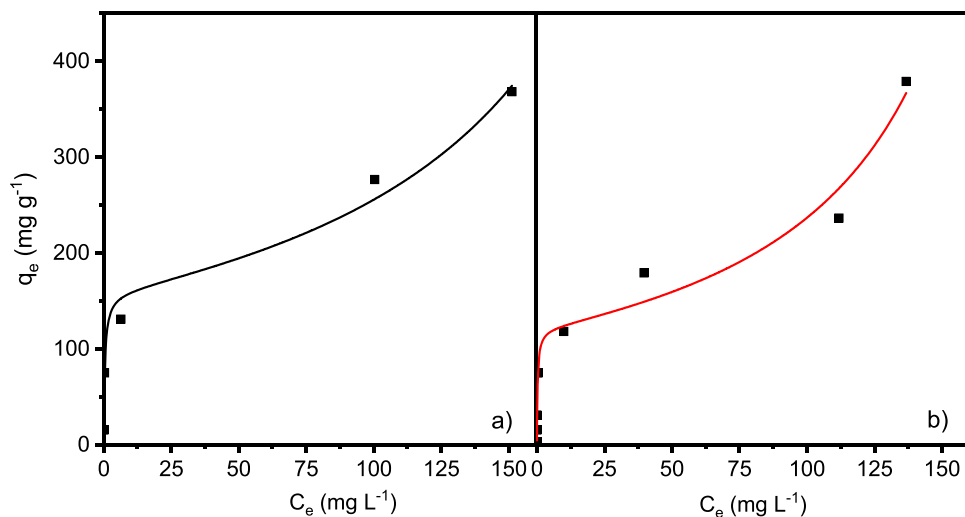
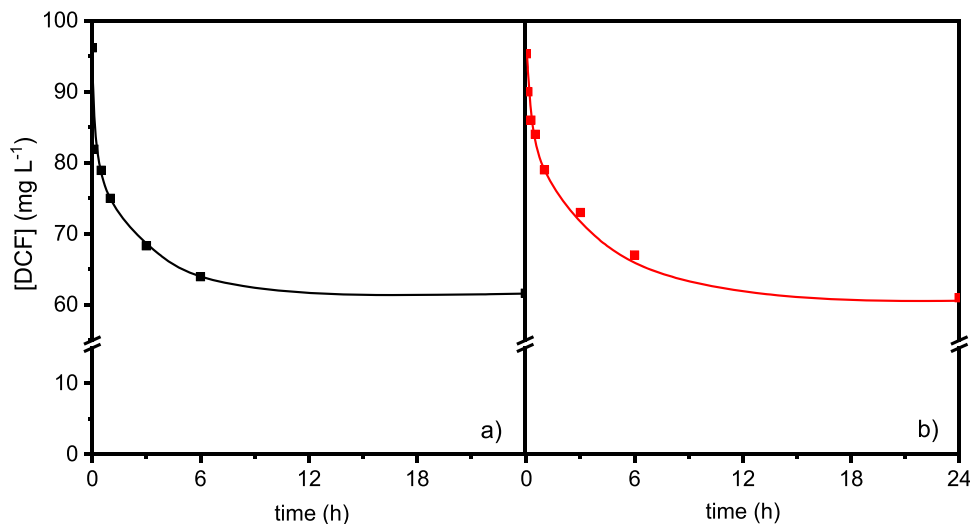


Fig. 2. Equilibrium adsorption isotherms of DCF onto a) GAC and b) Fe₃O₄/GAC ([DCF]₀ = 1–250 mg L⁻¹; [Adsorbent] = 0.3 mg mL⁻¹). Experimental (symbols) and fitted (solid lines).

Table 2Parameters of adsorption kinetics of DCF onto GAC and Fe₃O₄/GAC by Langmuir, Freundlich and GAB models.

	Langmuir model			Freundlich model			GAB model			
	q _{sat}	b	R ²	k _F	n _F	R ²	q _m	K ₁	K ₂	R ²
Fe ₃ O ₄ /GAC	480	0.0173	0.82	44.3	2.428	0.88	120	3.79	0.0049	0.97
GAC	326	0.9187	0.93	74.2	3.260	0.97	158	2.38	0.0038	0.98

**Fig. 3.** DCF adsorption over (a) GAC and (b) Fe₃O₄/GAC ([DCF]₀ = 100 mg L⁻¹; [Adsorbent] = 0.3 mg mL⁻¹).

comparison with other works that increased the Fe weight (Gu et al., 2021).

Different empirical adsorption models (Langmuir, Freundlich and Guggenheim-Anderson de Boer (GAB)) were applied to fit the experimental adsorption data. Following the equations described in the Supplementary Material, the model parameters were calculated (Table 2). The highest correlation coefficients were obtained applying the GAB model (> 0.96) for both GAC and Fe₃O₄/GAC materials. In fact, as showed in Fig. 2, GAB model successfully described the experimental adsorption data. This model is frequently used in the fitting of experimental multilayer isotherms (Álvarez-Torrellas et al., 2016). In both cases, a plateau was observed up to a threshold value of 10–100 mg L⁻¹ DCF concentration, indicating the monolayer completion. At higher concentrations, a clear sigmoidal trend was found, which can be related to the multilayer adsorption and vertical packing of the adsorbate molecules onto the adsorbent centers. The formation of several layers of the adsorbate is favored by higher pore size of the material (Álvarez-Torrellas et al., 2018) and smaller molecular size of the micropollutants (Munoz et al., 2021). Moreover, K₁ value was considerably higher than K₂, which demonstrated that the affinity to the first layer of DCF adsorbed is far greater than that of the second layer for both materials. On the other hand, both Langmuir and Freundlich models did not allow to describe the experimental data as they only assume the formation of a monolayer adsorbate onto the adsorbent surface (Munoz et al., 2021).

3.3. Adsorption kinetics

Once evaluated the adsorption capacity of the materials for DCF removal, a kinetic study was performed. The effect of contact time on DCF adsorption over GAC and Fe₃O₄/GAC was evaluated for 24 h at 25 °C. DCF initial concentration was established at 100 mg L⁻¹ and the adsorbent dose was fixed at 0.3 mg mL⁻¹. Fig. 3 shows the evolution of DCF along the adsorption experiments. In both cases, more than 75% of equilibrium uptake was achieved in 3 h, which allowed to confirm that the immobilization of magnetite nanoparticles onto the GAC surface did not affect its adsorption rate. The obtained results are consistent with those

previously reported in the literature for GAC materials (Bhadra et al., 2016; Piai et al., 2019; Zhao et al., 2019). Several hours are commonly required to reach the equilibrium for micropollutants removal over GAC materials.

The kinetic data were successfully described by the commonly applied pseudo-second order model, described by Ho (1995). The pseudo-second-order rate constant values obtained were 2.39 and 1.11 g mg⁻¹ h⁻¹ for GAC and Fe₃O₄/GAC, respectively, with correlation coefficients above 0.99 (see Fig. S4 of the Supplementary Material). Although somewhat lower kinetic constant was obtained for Fe₃O₄/GAC, it must be highlighted that even for the synthesized adsorbent the adsorption rate was much higher than those reported in the literature for micropollutants removal by other GAC materials. For instance, Bhadra et al. (2016) obtained rate constant values of 0.006 and 0.012 g mg⁻¹ h⁻¹ in the removal of 100 mg DCF L⁻¹ using commercial and oxidized GAC, respectively (Bhadra et al., 2016). On the other hand, the amount of solute adsorbed at equilibrium was 116 and 118 mg g⁻¹ for GAC and Fe₃O₄/GAC, respectively, which is consistent with the previously shown adsorption isotherm data.

3.4. Adsorbents regeneration and reuse

Once demonstrated the effectiveness of Fe₃O₄/GAC for DCF removal, which was quite close to the achieved by conventional GAC, adsorbent regeneration by heterogeneous Fenton oxidation was evaluated. Prior to this study, the adsorption capacity of the used adsorbents was also determined. As can be seen in the Supplementary Material (Fig. S5), the adsorption capacity of the saturated adsorbents dramatically decreased after being used (from 116 to 41 and from 121 to 44 mg g⁻¹ when GAC and Fe₃O₄/GAC were used, respectively) due to the reduction of the available adsorption sites. These somehow expected results allowed to confirm that adsorbents regeneration is imperative to allow their reusability.

The regeneration of the saturated adsorbents was carried via heterogeneous Fenton oxidation (H₂O₂ addition) operating at pH₀=3 and 25

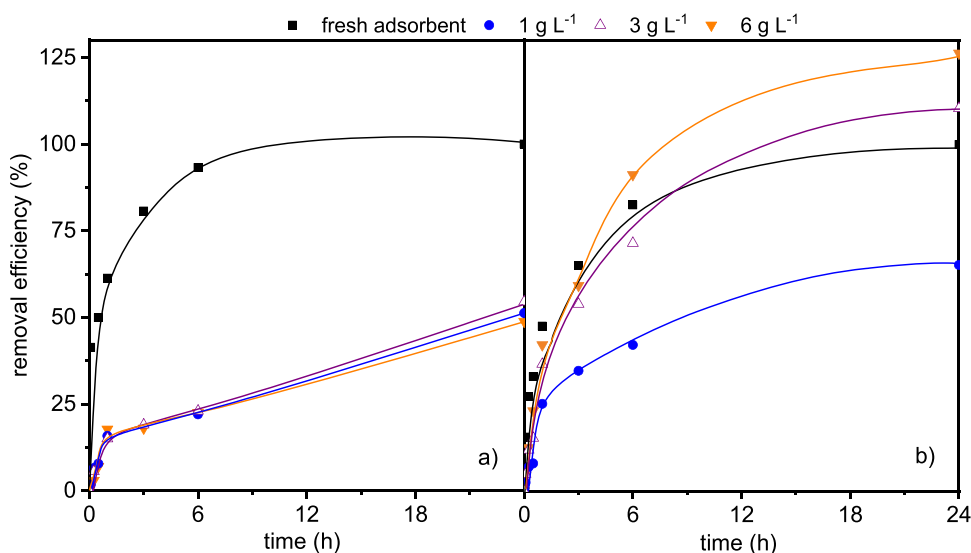


Fig. 4. DCF adsorption onto (a) GAC and (b) $\text{Fe}_3\text{O}_4/\text{GAC}$ after regeneration at different H_2O_2 doses. ($[\text{DCF}]_0 = 100 \text{ mg L}^{-1}$; $[\text{Adsorbent}] = 0.3 \text{ mg mL}^{-1}$).

^gC. The saturated adsorbents (0.25 g L^{-1}) were immersed into an aqueous H_2O_2 solution for 20 h. The effect of H_2O_2 concentration was evaluated within 1 to 6 g L^{-1} range. After regeneration, the adsorbents were used for a second adsorption run under the same operating conditions previously described. Fig. 4 shows the evolution of DCF concentration along the adsorption experiments before and after adsorbents regeneration at different H_2O_2 doses. As can be seen, complete regeneration of the $\text{Fe}_3\text{O}_4/\text{GAC}$ adsorption capacity was achieved using H_2O_2 doses at or above 3 g L^{-1} while conventional GAC only restored 50% of its adsorption capacity. In terms of kinetics, similar curves were achieved for regenerated and fresh $\text{Fe}_3\text{O}_4/\text{GAC}$ materials while a sharp decrease on the adsorption rate was observed in the case of GAC (See Table S1 of the Supplementary Material). Clearly, the presence of magnetite nanoparticles onto the GAC surface allowed the effective regeneration of $\text{Fe}_3\text{O}_4/\text{GAC}$ due to the generation of hydroxyl radicals from H_2O_2 , strong oxidizing species that allow to effectively remove the organic pollutants. It must be noted that in the case of $\text{Fe}_3\text{O}_4/\text{GAC}$, even slightly higher adsorption capacities than that of the fresh solid were achieved when the highest H_2O_2 dose was used. This fact could be due to the generation of carboxylic acids onto the carbon surface along regeneration, which could somehow favor the adsorption of DCF via hydrogen bonding. The presence of these acidic groups was confirmed by the low pH_{PZC} value of the regenerated adsorbent, which was close to 4 (see Fig. S6 of Supplementary Material). Regarding the stability of $\text{Fe}_3\text{O}_4/\text{GAC}$, it should be highlighted that iron leaching was below 2 mg L^{-1} during the regeneration process in all cases and was negligible along the adsorption experiments ($<0.1 \text{ mg L}^{-1}$).

Although Fenton-like processes have been previously explored for adsorbent regeneration (Díez et al., 2018; Santos et al., 2020), the few works published have dealt with the application of heterogeneous Fenton oxidation in batch mode (Table 3). Among them, high regeneration removal efficiencies have been reported but, complete regeneration has not been achieved in any case, even operating at mild temperatures or high H_2O_2 doses (Qin et al., 2014; Tong et al., 2016). Moreover, the consecutive application of adsorption-regeneration cycles generally has led to a decrease in regeneration efficiency. For instance, Duan et al. (2015) synthesized magnetic AC for the removal of 4-chlorophenol and after the application of the regeneration achieved 92% of adsorption capacity restored (Duan et al., 2020). However, a progressive decrease after successive adsorption/oxidation cycles was observed until achieving only 80% after the fifth application. Furthermore, continuous operation mode in long-term experiments have not been barely considered, which is essential for potential scale-up.

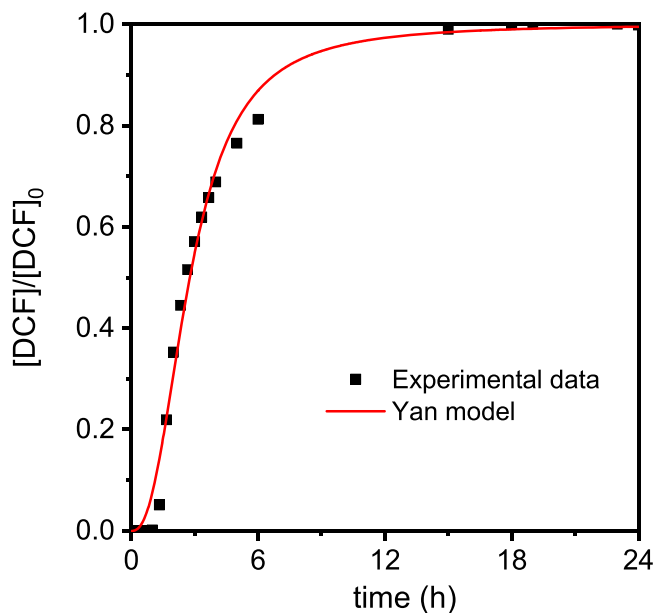


Fig. 5. Breakthrough curve of DCF removal by $\text{Fe}_3\text{O}_4/\text{GAC}$ packed column ($[\text{DCF}]_0 = 100 \text{ mg L}^{-1}$; $[\text{Adsorbent}] = 0.5 \text{ g}$; $Q = 3 \text{ mL min}^{-1}$). Experimental (symbols) and fitted (solid lines).

3.5. Continuous adsorption in fixed-bed column

A fixed-bed column packed by $\text{Fe}_3\text{O}_4/\text{GAC}$ ($d_p = 150\text{--}315 \text{ nm}$) was developed to investigate the performance of the material in continuous operation. In preliminary experiments (see Supplementary Material for further details), the reactor dimensions, bed weight and flow rate were optimized. A tubular quartz reactor with 4 and 1 mm of internal diameter and thickness, respectively, was employed. The bed weight was established at 0.5 g, corresponding to a bed length of 8.5 cm, and the volumetric flow rate at 3 mL min^{-1} . Under these operating conditions, the breakthrough curve showed in Fig. 5 was obtained. As can be observed, the breakthrough time at $C/C_0=0.05$ occurred at 40 min. Afterwards, the breakthrough curve became steeper, reaching the almost complete saturation at 15 h.

Table 3

Summary of the application of adsorption-heterogeneous Fenton regeneration on carbon adsorbents.

Mode	Adsorbent	Target pollutant	Operating conditions	Regeneration conditions	First cycle regeneration efficiency	Consecutive cycles	Refs.
Batch	Fe ₃ O ₄ /RGO	Rhodamine B (RhB)	[RhB]=50 mg L ⁻¹ [Ads]= 2 mg mL ⁻¹	[H ₂ O ₂]=1 g L ⁻¹ t=0.5 h T=50°C pH=3	95%	90% removal efficiency after 3 cycles	Qin et al. (2014)
	α-Fe ₂ O ₃ @PHCMs	Methyl Violet dye (MV)	[MV]=10–50 mg L ⁻¹ [Ads]= 0.25–1.25 mg mL ⁻¹	[H ₂ O ₂]=145 g L ⁻¹ t=0.5 h	95%	88% removal efficiency after 3 cycles	Tong et al. (2016)
	Fe ₃ O ₄ /AC	4-chlorophenol (4-CP)	[4-CP]=100 mg L ⁻¹ [Ads]= 0.3 mg mL ⁻¹	[H ₂ O ₂]=0.68 g L ⁻¹ t=6 h Fe ²⁺ /Fe ³⁺ =3:1 pH=3	96%	80% removal efficiency after 5 cycles	Duan et al. (2020)
	MagFePC-700	Tetracycline (TC)	[TC]=80 mg L ⁻¹ [Ads]= 0.05 mg mL ⁻¹	[H ₂ O ₂]=1.5 g L ⁻¹ t=4 h pH=6	96%	92.5% removal efficiency after 3 cycles	Gu et al. (2021)
Continuous	Fe ₃ O ₄ @yeastmicrospheres	Methylene blue dye (MB)	[MB]=100 mg L ⁻¹ Q=5 mL min ⁻¹ Bed depth=1.2 cm pH=7	[H ₂ O ₂]=100 g L ⁻¹ Q=1 mL min ⁻¹ t=1 h	99%	97% removal efficiency after 3 cycles	Song et al. (2015)
	SBC@β-FeOOH composites	Doxycycline (DC)	[DC]=27 mg L ⁻¹ Q=1 mL min ⁻¹ Bed depth=1.1 cm pH=6	[H ₂ O ₂]=50 g L ⁻¹ Q=1 mL min ⁻¹ t=2 h	90.6%	70% removal efficiency after 3 cycles	Zhang et al. (2016)
	Fe ₃ O ₄ @chitosan carbon microbeads	Doxycycline (DC)	[DC]=25 mg L ⁻¹ Q=1.1 mL min ⁻¹ Bed depth=1.2 cm pH=6	[H ₂ O ₂]=50 g L ⁻¹ Q=1.1 mL min ⁻¹ t=1.5 h	93%	65% removal efficiency after 3 cycles	Bai et al. (2018)

Yan model successfully described the breakthrough curve, obtaining a R² value of 0.99. Saturation adsorption capacity and rate constant values of 99.7 mg g⁻¹ and 2.44 were obtained, respectively. These results are consistent with those previously reported by [Katsigiannis et al. \(2015\)](#), who also found that Yan model was the most accurate mathematical model to describe the breakthrough curves obtained in the adsorption of a representative group of emerging pollutants by GAC ([Katsigiannis et al., 2015](#)).

3.6. Continuous adsorption-regeneration in fixed-bed column

To further prove the reusability of the Fe₃O₄/GAC adsorbent, consecutive adsorption-regeneration experiments were carried in the fixed-bed column. In this case, regeneration by heterogeneous Fenton oxidation was performed *in-situ* once the adsorbent reached the saturation. Taking into account the results obtained in the regeneration carried out in batch, a H₂O₂ dose of 6 g L⁻¹ at 3 mL min⁻¹ passed through the fixed-bed column during 3 h. Afterwards, a new breakthrough curve of DCF adsorption was obtained. Three consecutive adsorption/oxidation runs were carried out, as shown in [Fig. 6](#). In all cases, the adsorbent started to saturate at around 1 h (180 mL volume) and similar breakthrough curves were obtained. Yan model successfully described the breakthrough curves. The equilibrium adsorption capacities obtained were 99, 86 and 89 mg g⁻¹ for the first, second and third run respectively. It can be then confirmed that the adsorption capacity of the solid was restored via heterogeneous Fenton oxidation. Furthermore, the concentration of dissolved iron along the regeneration runs was low (< 0.5 mg L⁻¹) while along the adsorption runs the iron leached values were negligible (< 0.1 mg L⁻¹). All in all, the loss of iron from the solid after the three adsorption-regeneration cycles represented less than 2% wt. of the initial Fe content – calculated by measuring dissolved iron concentration in the adsorption and regeneration effluents– which proved its high stability.

To get further insights, a new set of adsorption/oxidation experiments were carried out to prove the feasibility of the system in the treatment of a representative concentration of DCF (500 µg L⁻¹). Same conditions than the previous fixed-bed column at high DCF concentration were employed, 0.5 g of bed weight and 3 mL min⁻¹ of volumetric flow rate. Under these operating conditions, the complete removal of

the pollutant was achieved along 10 days and the breakthrough time at C/C₀=0.05 occurred at 11 days. As expected, the breakthrough time was increased at lower inlet concentrations in comparison with the previous experiment as well as the slope of breakthrough curve became less steeper in this case ([Lin et al., 2017](#)). After reaching almost complete saturation (>95%), the adsorbent was treated for just 3 h using a H₂O₂ dose of 6 g L⁻¹ at 3 mL min⁻¹. Afterwards, a continuous DCF flow was introduced again into the fixed bed column and similar results were obtained in the breakthrough curve of a second adsorption run, achieving the complete removal of DCF along 10 days. Thus, short regeneration times (3 h) allowed to completely restore the adsorption capacity of Fe₃O₄/GAC in long-term experiments.

The results obtained in this work can be favorably compared with the few works reported in the literature dealing with the continuous mode *in-situ* regeneration of carbon adsorbents via heterogeneous Fenton oxidation (see [Table 3](#)). In this sense, again, regeneration removal efficiencies have suffered a remarkable decrease after consecutive adsorption-regeneration cycles in most reported works. For instance, [Zhang et al. \(2016\)](#) evaluated this regeneration method by the incorporation of FeOOH nanoparticles to a biocarbon for doxycycline removal. Three adsorption-regeneration cycles were carried out at the optimum H₂O₂ dose, but a progressively decrease of the regeneration efficiency up to 70% in the third run was observed, attributed to the stronger affinity of the intermediate products generated during the degradation process. Similar results were shown by [Bai et al. \(2018\)](#), with the incorporation of Fe₃O₄ on Chitosan carbon, leading to a progressively decrease of the removal efficiency in the consecutive adsorption-regeneration application. On the other hand, [Song et al. \(2015\)](#) showed 97% removal efficiency after three consecutive adsorption-regeneration cycles, but high H₂O₂ doses (up to 100 g L⁻¹) and Fe content (34.95%) were needed. In addition, a significant decrease, over 65%, in the adsorption capacity after the consecutive cycles was reported, attributed to the inability of the Fenton reaction to remove the target pollutant sorbed deeply into the cores, since Fe₃O₄ was primarily supported on the surface ([Song et al., 2015](#)). Furthermore, by the employment of other supports, iron leaching from the adsorbent material was also reported, which led to higher regeneration efficiencies by homogeneous Fenton oxidation contribution ([Shahbazi et al., 2014](#); [Xu et al., 2019](#)). All in all, these results demonstrates the promising application of the developed adsor-

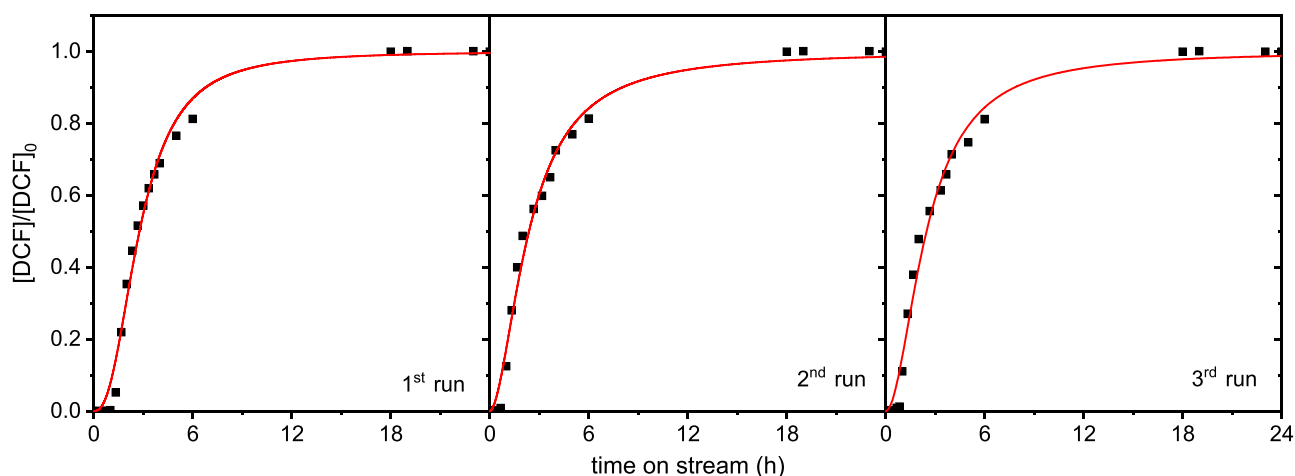


Fig. 6. Breakthrough curves of DCF removal by $\text{Fe}_3\text{O}_4/\text{GAC}$ after adsorption-oxidation runs. ($[\text{DCF}]_0 = 100 \text{ mg L}^{-1}$; $[\text{Adsorbent}] = 0.5 \text{ g}$; $Q = 3 \text{ mL min}^{-1}$). Experimental (symbols) and fitted (solid lines).

bent ($\text{Fe}_3\text{O}_4/\text{GAC}$) for the continuous adsorption and subsequent *in-situ* regeneration for micropollutants removal.

4. Conclusions

Granular activated carbon decorated with magnetite nanoparticles ($\text{Fe}_3\text{O}_4/\text{GAC}$), that allows the *in-situ* regeneration of the saturated solid through heterogeneous Fenton oxidation, was prepared. The adsorbent was prepared by the incorporation of 5% wt. iron to commercial GAC by incipient wetness impregnation followed by calcination and reduction steps. The incorporation of magnetite nanoparticles did not significantly modify neither the specific surface area ($\sim 1000 \text{ m}^2 \text{ g}^{-1}$) nor the main properties of the solid and its adsorption capacity for DCF removal remained practically unchanged ($\sim 400 \text{ mg g}^{-1}$). Remarkably, the addition of H_2O_2 allowed to restore the adsorption capacity of the adsorbent by the heterogeneous Fenton oxidation process at 25°C using a H_2O_2 dose of $3 - 6 \text{ g L}^{-1}$ during 20 h. The adsorption performance of the solid in continuous mode was evaluated in a fixed-bed column and the *in-situ* regeneration was notably demonstrated in three consecutive adsorption-regeneration runs. Remarkably, iron leaching was practically negligible during operation. Finally, the feasibility of the system was proved in the treatment of a diluted stream ($500 \mu\text{g L}^{-1}$ DCF), achieving the complete removal of the pollutant along 10 days and the adsorbent was effectively regenerated in just 3 h.

Data availability

No data was used for the research described in the article.

Acknowledgments

This research has been supported by the Spanish MINECO thorough the projects PCI2020-112013 and PID2019-105079RB-I00 and by the CM through the project P2018/EMT-4341. J. Nieto-Sandoval and N. Lopez-Arago thank the Spanish MINECO for the FPI grant (BES-2017-081346) and FPI predoctoral grant (PRE2020-094527), respectively. M. Munoz thanks the Spanish MINECO for the Ramón y Cajal postdoctoral contract (RYC-2016-20648).

Supplementary materials

Supplementary material associated with this article can be found, in the online version, at doi:10.1016/j.hazadv.2023.100267.

References

- Acuña, V., Ginebreda, A., Mor, J.R., Petrovic, M., Sabater, S., Sumpter, J., Barceló, D., 2015. Balancing the health benefits and environmental risks of pharmaceuticals: diclofenac as an example. *Environ. Int.* 85, 327–333. doi:10.1016/j.envint.2015.09.023.
- Altmann, J., Rehfeld, D., Träder, K., Sperlich, A., Jekel, M., 2016. Combination of granular activated carbon adsorption and deep-bed filtration as a single advanced wastewater treatment step for organic micropollutant and phosphorus removal. *Water Res.* 92, 131–139. doi:10.1016/j.watres.2016.01.051.
- Álvarez-Torrellas, S., Rodríguez, A., Ovejero, G., García, J., 2016. Comparative adsorption performance of ibuprofen and tetracycline from aqueous solution by carbonaceous materials. *Chem. Eng. J.* 283, 936–947. doi:10.1016/j.cej.2015.08.023.
- Álvarez-Torrellas, S., Munoz, M., Gläsel, J., de Pedro, Z.M., Domínguez, C.M., García, J., Casas, J.A., 2018. Highly efficient removal of pharmaceuticals from water by well-defined carbide-derived carbons. *Chem. Eng. J.* 347, 595–606. doi:10.1016/j.cej.2018.04.127.
- Bai, B., Xu, X., Li, C., Xing, J., Wang, H., Suo, Y., 2018. Magnetic $\text{Fe}_3\text{O}_4/\text{Chitosan}$ carbon microbeads: removal of doxycycline from aqueous solutions through a fixed bed via sequential adsorption and heterogeneous Fenton-like regeneration. *J. Nanomater.* 5296410. doi:10.1155/2018/5296410.
- Barbosa, M.O., Moreira, N.F.F., Ribeiro, A.R., Pereira, M.F.R., Silva, A.M.T., 2016. Occurrence and removal of organic micropollutants: an overview of the watch list of EU decision 2015/495. *Water Res.* 94, 257–279. doi:10.1016/j.watres.2016.02.047.
- Bhadra, B.N., Seo, P.W., Jung, S.H., 2016. Adsorption of diclofenac sodium from water using oxidized activated carbon. *Chem. Eng. J.* 301, 27–34. doi:10.1016/j.cej.2016.04.143.
- Blahovec, J., Yanniotis, S., 2009. Modified classification of sorption isotherms. *J. Food Eng.* 72–77. doi:10.1016/j.jfoodeng.2008.08.007.
- Bohart, G.S., Adams, E.Q., 1920. Some aspects of the behavior of charcoal with respect to chlorine. *J. Am. Chem. Soc.* 42 (3), 523–544. doi:10.1021/ja01448a018.
- Bolong, N., Ismail, A.F., Salim, M.R., Matsuura, T., 2009. A review of the effects of emerging contaminants in wastewater and options for their removal. *Desalination* 239 (1), 229–246. doi:10.1016/j.desal.2008.03.020.
- Cai, Q.Q., Wu, M.Y., Hu, L.M., Lee, B.C.Y., Ong, S.L., Wang, P., Hu, J.Y., 2020. Organics removal and *in-situ* granule activated carbon regeneration in FBR-Fenton/GAC process for reverse osmosis concentrate treatment. *Water Res.* 183, 116119. doi:10.1016/j.watres.2020.116119.
- de Andrade, J.R., Oliveira, M.F., Canevesi, R.L.S., Landers, R., Silva, da, Meuris, C., Vieira, M.G.A., 2020. Comparative adsorption of diclofenac sodium and losartan potassium in organophilic clay-packed fixed-bed: x-ray photoelectron spectroscopy characterization, experimental tests and theoretical study on DFT-based chemical descriptors. *J. Mol. Liq.* 312, 113427. doi:10.1016/j.molliq.2020.113427.
- Diez, A.M., Sanromán, M.A., Pazos, M., 2018. Fenton-based processes for the regeneration of catalytic adsorbents. *Catal. Today* 313, 122–127. doi:10.1016/j.cattod.2017.10.030.
- Duan, Z., Zhang, W., Lu, M., Shao, Z., Huang, W., Li, J., Chen, C., 2020. Magnetic Fe_3O_4 /activated carbon for combined adsorption and Fenton oxidation of 4-chlorophenol. *Carbon N Y* 167, 351–363. doi:10.1016/j.carbon.2020.05.106.
- Gomes, H.T., Miranda, S.M., Sampaio, M.J., Silva, A.M.T., Faria, J.L., 2010. Activated carbons treated with sulphuric acid: catalysts for catalytic wet peroxide oxidation. *Catal. Today* 151 (1), 153–158. doi:10.1016/j.cattod.2010.01.017.
- Gu, W., Huang, X., Tian, Y., Cao, M., Zhou, L., Zhou, Y., Zhang, J., 2021. High-efficiency adsorption of tetracycline by cooperation of carbon and iron in a magnetic Fe/porous carbon hybrid with effective Fenton regeneration. *Appl. Surf. Sci.* 538, 147813. doi:10.1016/j.apsusc.2020.147813.
- Guillossou, R., Le Roux, J., Mailler, R., Vulliet, E., Morlay, C., Nauleau, F., Rocher, V., 2019. Organic micropollutants in a large wastewater treatment plant: what are the benefits of an advanced treatment by activated carbon adsorp-

- tion in comparison to conventional treatment? *Chemosphere* 218, 1050–1060. doi:10.1016/j.chemosphere.2018.11.182.
- Hasan, Z., Khan, N.A., Jhung, S.H., 2016. Adsorptive removal of diclofenac sodium from water with Zr-based metal-organic frameworks. *Chem. Eng. J.* 284, 1406–1413. doi:10.1016/j.cej.2015.08.087.
- Hernández-Abreu, A.B., Álvarez-Torrellas, S., Águeda, V.I., Larriba, M., Delgado, J.A., Calvo, P.A., García, J., 2020. New insights from modelling and estimation of mass transfer parameters in fixed-bed adsorption of bisphenol A onto carbon materials. *J. Contam. Hydrol.* 228, 103566. doi:10.1016/j.jconhyd.2019.103566.
- Ho, Y.S., McKay, G., 1999. Pseudo-second order model for sorption processes. *Process Biochem.* 34 (5), 451–465. doi:10.1016/S0032-9592(98)00112-5.
- Ho, Y., 1995. *Absorption of Heavy Metals from Waste Streams by Peat*. University of Birmingham Ph.D.1995.
- Kårelid, V., Larsson, G., Björleinius, B., 2017. Pilot-scale removal of pharmaceuticals in municipal wastewater: comparison of granular and powdered activated carbon treatment at three wastewater treatment plants. *J. Environ. Manage.* 193, 491–502. doi:10.1016/j.jenvman.2017.02.042.
- Katsigiannis, A., Noutsopoulos, C., Mantziaras, J., Gioldasi, M., 2015. Removal of emerging pollutants through granular activated carbon. *Chem. Eng. J.* 280, 49–57. doi:10.1016/j.cej.2015.05.109.
- Khan, S., Naushad, M., Govarthanan, M., Iqbal, J., Alfadul, S.M., 2022. Emerging contaminants of high concern for the environment: current trends and future research. *Environ. Res.* 207, 112609. doi:10.1016/j.envres.2021.112609.
- Larasati, A., Fowler, G.D., Graham, N.J.D., 2020. Chemical regeneration of granular activated carbon: preliminary evaluation of alternative regenerant solutions. *Environ. Sci. Water Res. Technol.* 6 (8), 2043–2056. doi:10.1039/D0EW00328J.
- Lin, X., Huang, Q., Qi, G., Shi, S., Xiong, L., Huang, C., Chen, X., 2017. Estimation of fixed-bed column parameters and mathematical modeling of breakthrough behaviors for adsorption of levulinic acid from aqueous solution using SY-01 resin. *Sep. Purif. Technol.* 174, 222–231. doi:10.1016/j.seppur.2016.10.016.
- Lu, P., Lin, H., Yu, W., Chern, J., 2011. Chemical regeneration of activated carbon used for dye adsorption. *J. Taiwan Inst. Chem. Eng.* 42 (2), 305–311. doi:10.1016/j.jtice.2010.06.001.
- Luo, Y., Guo, W., Ngo, H.H., Long Duc, N., Hai, F.I., Zhang, J., Wang, X.C., 2014. A review on the occurrence of micropollutants in the aquatic environment and their fate and removal during wastewater treatment. *Sci. Total Environ.* 473, 619–641. doi:10.1016/j.scitotenv.2013.12.065.
- Munoz, M., de Pedro, Z.M., Menendez, N., Casas, J.A., Rodriguez, J.J., 2013. A ferromagnetic γ -alumina-supported iron catalyst for CWPO. Application to chlorophenols. *Appl. Catal. B: Environ.* 136–137, 218–224. doi:10.1016/j.apcatb.2013.02.002.
- Munoz, M., Nieto-Sandoval, J., Álvarez-Torrellas, S., Sanz-Santos, E., Calderón, B., de Pedro, Z.M., Casas, J.A., 2021. Carbon-encapsulated iron nanoparticles as reusable adsorbents for micropollutants removal from water. *Sep. Purif. Technol.* 257, 117974. doi:10.1016/j.seppur.2020.117974.
- Pereira, L.C., de Souza, A.O., Franco Bernardes, M.F., Pazin, M., Tasso, M.J., Pereira, P.H., Dorta, D.J., 2015. A perspective on the potential risks of emerging contaminants to human and environmental health. *Environ. Sci. Pollut. Res. Int.* 22 (18), 13800–13823. doi:10.1007/s11356-015-4896-6.
- Piai, L., Dykstra, J.E., Adishakti, M.G., Blokland, M., Langenhoff, A.A.M., van der Wal, A., 2019. Diffusion of hydrophilic organic micropollutants in granular activated carbon with different pore sizes. *Water Res.* 162, 518–527. doi:10.1016/j.watres.2019.06.012.
- Qin, Y., Long, M., Tan, B., Zhou, B., 2014. RhB adsorption performance of magnetic adsorbent $\text{Fe}_3\text{O}_4/\text{RGO}$ composite and its regeneration through A Fenton-like reaction. *Nanomicro Lett.* 6 (2), 125–135. doi:10.1007/BF03353776.
- Rakić, V., Rac, V., Krmar, M., Otman, O., Auroux, A., 2015. The adsorption of pharmaceutically active compounds from aqueous solutions onto activated carbons. *J. Hazard. Mater.* 282, 141–149. doi:10.1016/j.jhazmat.2014.04.062.
- Rizzo, L., Malato, S., Antakylis, D., Beretsou, V.G., Đolić, M.B., Gernjak, W., Fatta-Kassinos, D., 2019. Consolidated vs new advanced treatment methods for the removal of contaminants of emerging concern from urban wastewater. *Sci. Total Environ.* 655, 986–1008. doi:10.1016/j.scitotenv.2018.11.265.
- Rodriguez-Narvaez, O.M., Peralta-Hernandez, J.M., Goonetilleke, A., Andala, E.R., 2017. Treatment technologies for emerging contaminants in water: a review. *Chem. Eng. J.* 323, 361–380. doi:10.1016/j.cej.2017.04.106.
- Rout, P.R., Zhang, T.C., Bhunia, P., Surampalli, R.Y., 2021. Treatment technologies for emerging contaminants in wastewater treatment plants: a review. *Sci. Total Environ.* 753, 141990. doi:10.1016/j.scitotenv.2020.141990.
- Sandell, E.B., 1959. *Colorimetric Determination of Traces of Metals*. Interscience Publishers, Inc., New York 1959.
- Santos, D.H.S., Duarte, J.L.S., Tonholo, J., Meili, L., Zanta, C.L.P.S., 2020. Saturated activated carbon regeneration by UV-light, H_2O_2 and Fenton reaction. *Sep. Purif. Technol.* 250, 117112. doi:10.1016/j.seppur.2020.117112.
- Sathishkumar, P., Meena, R.A.A., Palanisami, T., Ashokkumar, V., Palvannan, T., Gu, F.L., 2020. Occurrence, interactive effects and ecological risk of diclofenac in environmental compartments and biota - a review. *Sci. Total Environ.* 698, 134057. doi:10.1016/j.scitotenv.2019.134057.
- Shahbazi, A., Gonzalez-Olmos, R., Kopinke, F., Zarabadi-Poor, P., Georgi, A., 2014. Natural and synthetic zeolites in adsorption/oxidation processes to remove surfactant molecules from water. *Sep. Purif. Technol.* 127, 1–9. doi:10.1016/j.seppur.2014.02.021.
- Shahid, M.K., Kashif, A., Fuwad, A., Choi, Y., 2021. Current advances in treatment technologies for removal of emerging contaminants from water – a critical review. *Coord. Chem. Rev.* 442, 213993. doi:10.1016/j.ccr.2021.213993.
- Song, R., Bai, B., Puma, G.L., Wang, H., Suo, Y., 2015. Biosorption of Azo dyes by raspberry-like Fe_3O_4 @yeast magnetic microspheres and their efficient regeneration using heterogeneous Fenton-like catalytic processes over an up-flow packed reactor. *React. Kinet. Mech. Catal.* 115 (2), 547–562. doi:10.1007/s11444-015-0854-z.
- Tan, I.A.W., Ahmad, A.L., Hameed, B.H., 2009. Fixed-bed adsorption performance of oil palm shell-based activated carbon for removal of 2,4,6-trichlorophenol. *Bioresour. Technol.* 100 (3), 1494–1496. doi:10.1016/j.biortech.2008.08.017.
- Thomas, H.C., 1944. Heterogeneous ion exchange in a flowing system. *J. Am. Chem. Soc.* 66 (10), 1664–1666. doi:10.1021/ja01238a017.
- Tong, Z., Zheng, P., Bai, B., Wang, H., Suo, Y., 2016. Adsorption performance of methyl violet via $\alpha\text{-Fe}_2\text{O}_3$ @Porous hollow carbonaceous microspheres and its effective regeneration through a Fenton-like reaction. *Catalysts* 6. doi:10.3390/catal6040058.
- von Gunten, U., 2018. Oxidation processes in water treatment: are we on track? *Environ. Sci. Technol.* 52 (9), 5062–5075. doi:10.1021/acs.est.8b00586.
- Wang, Y., Lin, C., Liu, X., Ren, W., Huang, X., He, M., Ouyang, W., 2021. Efficient removal of acetochlor pesticide from water using magnetic activated carbon: adsorption performance, mechanism, and regeneration exploration. *Sci. Total Environ.* 778, 146353. doi:10.1016/j.scitotenv.2021.146353.
- Xu, X., Chen, W., Zong, S., Ren, X., Liu, D., 2019. Magnetic clay as catalyst applied to organics degradation in a combined adsorption and Fenton-like process. *Chem. Eng. J.* 373, 140–149. doi:10.1016/j.cej.2019.05.030.
- Yan, G., Viraraghavan, T., Chen, M., 2001. A new model for heavy metal removal in a biosorption column. *Adsorp. Sci. Technol.* 19 (1), 25–43. doi:10.1260/0263617011493.
- Yin, R., Shang, C., 2020. Removal of micropollutants in drinking water using UV-LED/chlorine advanced oxidation process followed by activated carbon adsorption. *Water Res.* 185, 116297. doi:10.1016/j.watres.2020.116297.
- Zhang, X., Bai, B., Li Puma, G., Wang, H., Suo, Y., 2016. Novel sea buckthorn biocarbon SBC@ $\beta\text{-FeOOH}$ composites: efficient removal of doxycycline in aqueous solution in a fixed-bed through synergistic adsorption and heterogeneous Fenton-like reaction. *Chem. Eng. J.* 284, 698–707. doi:10.1016/j.cej.2015.09.012.
- Zhao, Y., Cho, C.W., Cui, L., Wei, W., Cai, J., Wu, G., Yun, Y.S., 2019. Adsorptive removal of endocrine-disrupting compounds and a pharmaceutical using activated charcoal from aqueous solution: kinetics, equilibrium, and mechanism studies. *Environ. Sci. Pollut. Res. Int.* 26 (33), 33897–33905. doi:10.1007/s11356-018-2617-7.
- Zhou, W., Meng, X., Gao, J., Zhao, H., Zhao, G., Ma, J., 2021. Electrochemical regeneration of carbon-based adsorbents: a review of regeneration mechanisms, reactors, and future prospects. *Chem. Eng. J. Adv.* 5, 100083. doi:10.1016/j.cej.2020.100083.